Proceedings of ICRC 2001: 435 © Copernicus Gesellschaft 2001

ICRC 2001

The influence of baryon stopping on cosmic ray showers

J. Ranft[1], **R. Engel**[2], **and S. Roesler**[3]

[1]Physics Dept. Universität Siegen, D–57068 Siegen, Germany
[2]University of Delaware, Bartol Research Institute, Newark DE 19716, USA
[3]SLAC, P.O. Box 20450, Stanford CA 94309, USA

Abstract. A new feature of hadron production in nuclear collisions is the large stopping of the participating nucleons. Experimental data demonstrating this effect have been presented by the NA35 Collaboration at the CERN SPS. In order to incorporate the effect into multichain models, new diquark breaking diagrams were proposed in Kharzeev (1996); Capella and Kopeliovich (1996). The new diagrams were investigated in Ranft (2000), where also their implementation into multistring fragmentation models was discussed. The presence of the new baryon stopping diagrams modifies considerably the extrapolation of multistring models to Cosmic Ray energies. The energy fractions carried by baryons decrease as compared to those obtained with models without the new diagrams.

1 Introduction

A recently discovered feature of hadron production in nuclear collisions is the large stopping of the participating nucleons in hadron–nucleus and nucleus–nucleus collisions. Experimental data demonstrating the large stopping of the participating nucleons in hadron–nucleus and nucleus–nucleus collisions have been presented in Alber et al. (1994) and Alber et al. (1998). Multistring fragmentation models like the Dual Parton Model (DPM) or similar models did originally not show this enhanced stopping in nuclear collisions. Therefore, in order to incorporate the effect into multistring fragmentation models new diquark breaking DPM–diagrams acting in hadron–nucleus and nucleus–nucleus collisions were proposed by Kharzeev (1996) and Capella and Kopeliovich (1996) and investigated in detail by Capella et al. (1999) and Capella and Salgado (1999). Similar ideas were discussed by Vance and Gyulassy (1999) and by Casado (1999). The Monte Carlo implementation into DPMJET–II.5 of the new diquark breaking diagrams of Kharzeev (1996) and Capella and Kopeliovich (1996) was first discussed by Ranft (2000).

Correspondence to: J. Ranft (Johannes.Ranft@cern.ch)

The implementation into DPMJET–III (Roesler et al., 2001) of these diagrams differs somewhat from that of Ranft (2000) and is described here.

2 Baryon stopping in multichain models

The new diquark breaking DPM–diagrams can be classified as (for details see (Ranft, 2000))

(i) GSQBS, the Glauber sea quark mechanism of baryon stopping, this diagram acts in nuclear collisions already at low energy.

(ii) USQBS, the unitary sea quark mechanism of baryon stopping, this mechanism leads to baryon stopping also in proton–proton collisions at collider and cosmic ray energies.

In DPMJET–III first the system of parton chains (strings) is constructed according to the model without the diquark breaking diagrams. This system is then searched for configurations of the type (i) as plotted on the left hand side of Fig. 1 or type (ii) (not shown, see below), where the left lower diquark is replaced by an antiquark. On the left hand side in Fig. 1 we have a diquark–quark chain and a sea quark–diquark chain with the (upper) diquark and seaquark belonging to the same projectile hadron and also the (lower) diquark and valence–quark belonging to the same target–nucleon. Configuration (ii) is characterized by a diquark–quark chain and a seaquark–anti–seaquark chain, with the (upper) diquark and seaquark belonging to the same projectile hadron and also the (lower) anti–seaquark and valence–quark belonging to the same target–nucleon. The chain system is transformed as shown on the right hand side of Fig. 1. The projectile diquark is split and the two resulting quarks come to the upper ends of both chains and the projectile seaquark goes into the middle of the second chain and determines the position where the baryon is produced. The sea quarks in Fig. 1 might be Glauber sea quarks or unitary sea quarks.

Besides the situations already discussed we consider also the splitting of target diquarks as well as the splitting of anti–

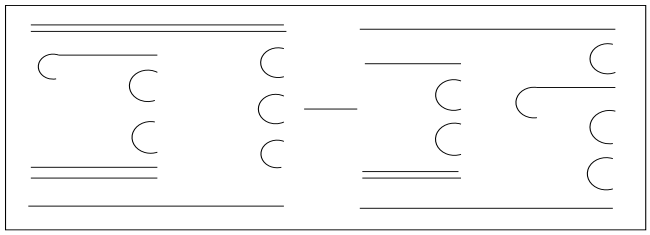

Fig. 1. Diquark breaking in an original diquark–quark and seaquark–diquark chain system.

diquarks.

The diquark is split by sampling for one of the two resulting valence quarks (randomly chosen) a normal valence quark momentum fraction x_{v1} and giving to the second valence quark the momentum fraction $x_{v2} = x_d - x_{v1}$, where x_d is the momentum fraction of the original diquark. For each of the new diquark breaking diagrams (GSQBS and USQBS) we have to introduce a new parameter. These parameters give the probability for the diquark breaking mechanisms to occur, given a suitable sea quark is available and given that the diquark breaking mechanism is kinematically allowed. For an original diquark–quark chain of small invariant mass, which originally just fragments into two hadrons, the diquark breaking is often not allowed. The optimum values of the new parameters are determined by comparing DPMJET–III with experimental data on net–baryon distributions. We obtain for the GSQBS parameters the value 0.6. The parameter for the USQBS diagrams could be determined from p–p collision data but no suitable data are available presently, therefore, we use the same value as for the GSQBS diagrams.

3 Comparison to data

Introducing the new baryon stopping mechanisms into DPMJET we get an significant modification of the model in different sectors: (i) The Feynman–x distributions of leading protons in proton–proton and proton–nucleus collisions. The leading particle production is especially important for the cosmic ray cascade simulation. (ii) The net–p ($p - \bar{p}$) and net–Λ ($\Lambda - \bar{\Lambda}$) rapidity distributions in hadron–nucleus and nucleus–nucleus collisions. These are the data on the enhanced baryon stopping mentioned already above. (iii) $\bar{p}/p$ and $\bar{\Lambda}/\Lambda$ ratios in the central region of heavy ion collisions. (iv) The production of hyperons and anti–hyperons in nuclear collisions. We present here examples for (i), (ii) and (iii).

3.1 x_{lab} distributions of leading protons

In Fig. 2 we compare the distribution in the energy fraction x_{lab} carried by the leading proton. The data are photoproduction and DIS measurements from the HERA collider at $\sqrt{s} \approx$ 200 GeV (Solano, 2000). The production of leading protons in the proton fragmentation region is not expected to depend strongly on the reaction channel. Therefore we can compare the $\gamma^\star$-p data to DPMJET–III for p-p interactions. We present the DPMJET–III distributions for the models with and without the diquark breaking diagrams (labeled "No Sto" in the plot). The models with and without the stopping diagrams are consistent with the measurements. The new diagrams modify the distributions mainly at intermediate x_{lab} values where no experimental data exist at present.

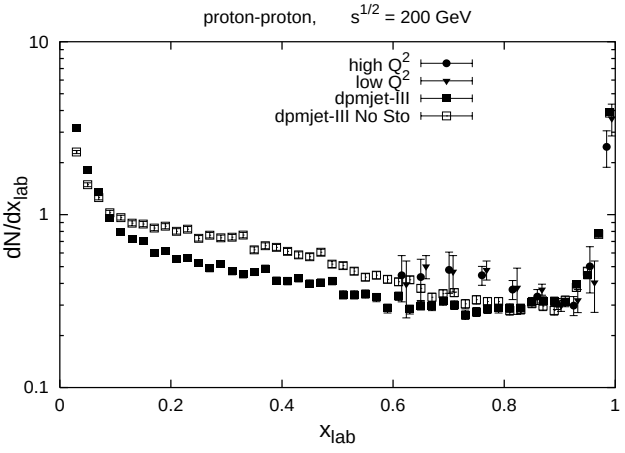

Fig. 2. Energy fraction x_{lab} carried by the leading proton. The data are photoproduction and DIS measurements at $\sqrt{s} \approx 200$ GeV (Solano, 2000) compared to DPMJET–III with and without (No Sto) the diquark breaking diagrams for p–p collisions at $\sqrt{s}$ = 200 GeV.

3.2 Net–proton distributions in hadron–nucleus and nucleus–nucleus collisions

In Fig. 3 we compare the net–proton distributions according to the models with and without the diquark breaking diagrams with data in p–Au collisions (Alber et al., 1998). The dip at central rapidity, which occurs in the model without the baryon stopping diagrams is filled. The full model follows the relatively flat distribution at central rapidities shown by the data.

In Fig. 4 we compare the DPMJET–III model with and without the diquark breaking diagrams with data on net–proton production in central S–S collisions. Also here the significant dip at central rapidity in the model without the new diagrams is much less pronounced in the full model, however, the agreement to the data of Alber et al. (1998) is not perfect.

3.3 Antibaryon/baryon ratios in nucleus–nucleus collisions at RHIC energies

So far all experimental evidence for enhanced baryon stopping results from SPS–experiments at energies E_{lab}=200 A-GeV. For cosmic ray applications we have the important question: is the enhanced baryon stopping an effect acting only at relatively low energies or is it independent from the collision energy. First data from the RHIC accelerator for Au–Au

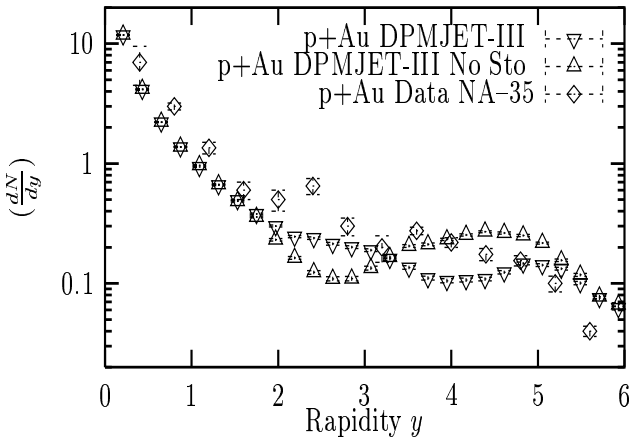

Fig. 3. Net proton ($p - \bar{p}$) rapidity distribution in p–Au collisions. The DPMJET–III results with and without (No Sto) the diquark breaking diagrams are compared with data (Alber et al., 1998).

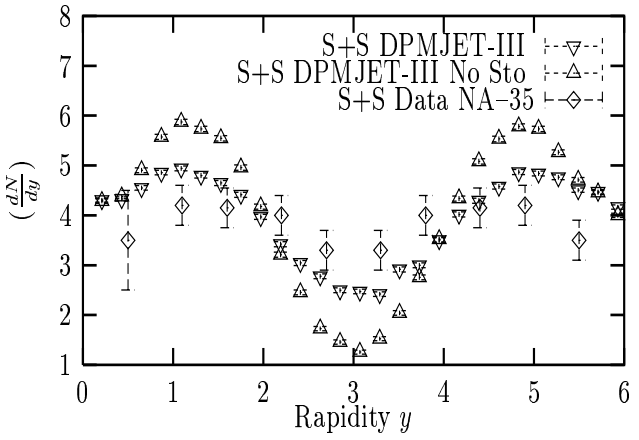

Fig. 4. Net proton ($p - \bar{p}$) rapidity distribution in central S–S collisions. The DPMJET–III results with and without (No Sto) the diquark breaking diagrams are compared with data (Alber et al., 1998).

collisions at $\sqrt{s}$= 130 A GeV are important to answer this question.

Let us discuss RHIC–data on the average charged multiplicity N_{ch} and the pseudorapidity plateau and preliminary RHIC–data on antibaryon/baryon ratios.

We have to discuss the average charged multiplicity N_{ch} and the pseudorapidity plateau in central Au–Au collisions mainly in order to prove that conventional multistring models still work under the RHIC conditions. The first data on the central pseudorapidity plateau at RHIC came from the PHOBOS Collaboration (Bach et al., 2000) : $dN_{ch}/d\eta_{\eta=0}$= 555 $\pm$12(stat)$\pm$35(syst) for the 6% most central collisions. The PHENIX Collaboration (Adcox et al., 2000) gave the plateau $dN_{ch}/d\eta_{\eta=0}$= 622 for the 1–5 % most central collisions. Finally there is the preliminary result from PHOBOS (Roland, 2001) N_{ch}=4100 $\pm$ 410 for the 3% most central collisions. DPMJET–III originally gave for central Au–Au collisions N_{ch} and the pseudorapidity plateau about 30 percent higher than the RHIC measurements. Shadowing corrections in dense nuclear matter are needed to correct the model. At the moment we use a simple effective method to obtain agreement with the RHIC measurements. The space in this contribution does not allow a detailed comparison to the RHIC data, we will discuss this comparison elsewhere. We also plan to start more serious work on shadowing for DPMJET-III.

Let us turn to $\bar{p}/p$ and $\bar{\Lambda}/\Lambda$ ratios. Preliminary data for Au–Au collisions at $\sqrt{s}$ = 130 A GeV were first presented at the Quark Matter Meeting 2001 by the BRAHMS Collaboration (Bearden, 2001), the STAR Collaboration (Huang, 2001) and the PHENIX Collaboration (Ohnishi, 2001). The particle ratios are found to be nearly independent on the transverse momentum and on the centrality of the collision (only a slight decrease of the ratios is found with the collision becoming more central). In the central region (rapidities y_{cms} = 0–0.4) and for central collisions the $\bar{p}/p$ ratio is found in the experiments to be 0.6 to 0.65. The STAR Collaboration gives for the $\bar{\Lambda}/\Lambda$ ratio 0.72 for the 15 % most central collisions. In DPMJET–III without the baryon stopping diagrams we find for the 5 % most central collisions in the central rapydity region $\bar{p}/p$=0.77–0.80 and $\bar{\Lambda}/\Lambda$=0.92-0.94 for $y_{cms} = 0 - 0.4$. This is clearly outside the RHIC–data. If we switch on the baryon stopping diagrams with the same parameters as described above, the stopping increases the proton and Lambda densities in the central region, the changes in the central antiproton densities are rather unimportant, the changes in the central anti–Lambda densities are more important than for antiprotons but less important than for Lambdas. Consequently the $\bar{p}/p$ and $\bar{\Lambda}/\Lambda$ ratios decrease. We find in the central region in the model with baryon stopping $\bar{p}/p$=0.60–0.64 and $\bar{\Lambda}/\Lambda$=0.64-0.70, the range of the ratios given corresponds to calculations performed with some slightly different DPMJET parameters. This agrees rather well with the preliminary RHIC–data.

We conclude from this agreement: the baryon stopping acts also at higher energy, therefore, we are encouraged to use the model with the baryon stopping diagrams also at cosmic ray energies.

4 Properties of the model at cosmic ray energies

The presence of the new baryon stopping diagrams modifies also the extrapolation of multistring models to cosmic ray energies. The energy fractions carried by baryons decrease relative to those predicted by models without the new diagrams. The energy fractions carried by mesons and the spectrum weighted moments of mesons increase as compared to models without the new diagrams. In the following we present model predictions for two important quantities calculated with and without stopping diagrams. All plots are for p–p collisions, the model behaves in a rather similar way also for p–air collisions. We first discuss plots, where the baryon stopping

mechanism causes significant differences.

The cosmic ray spectrum–weighted moments are defined as moments of x_{lab} distribution for the production of secondary particles i in hadron–hadron and hadron–nucleus collisions

$$F_i(x_{lab}) = x_{lab}\frac{dN_i}{dx_{lab}} \quad (1)$$

as follows

$$f_i = \int_0^1 (x_{lab})^{\gamma-1} F_i(x_{lab}) dx_{lab}. \quad (2)$$

Here $-\gamma \simeq$ –1.7 is the power of the integral cosmic ray energy spectrum. The spectrum–weighted moments for nucleon–air collisions, as discussed in Gaisser (1990), determine the uncorrelated fluxes of energetic particles in the atmosphere.

We also introduce the energy fraction K_i :

$$K_i = \int_0^1 F_i(x_{lab}) dx_{lab} \quad (3)$$

As for x_{lab}, the upper limit for K is 1 in hadron-hadron and hadron–nucleus collisions.

In Fig. 5 we present the spectrum weighted moments for charged pions in p–p collisions as function of the cms energy $\sqrt{s}$.

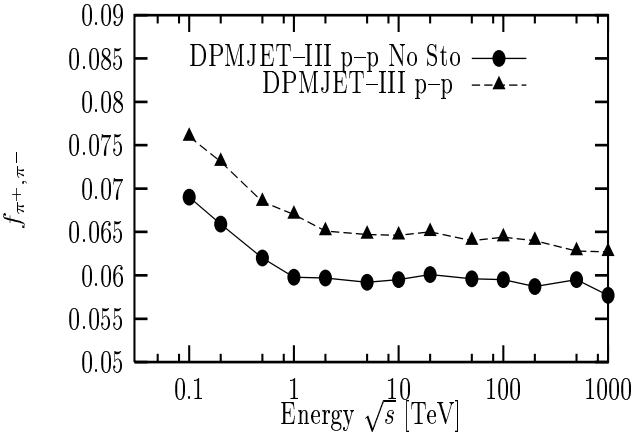

Fig. 5. Spectrum weighted moments for charged pion production in p–p collisions as function of the cms energy $\sqrt{s}$.

In Fig. 6 we present again for pp collisions the energy fraction K for net baryons $B - \bar{B}$ (baryon minus antibaryon). The difference between $K_{B-\bar{B}}$ and K_B is the energy fraction going into antibaryons $K_{\bar{B}}$ which is equal to the energy fraction carried by the baryons which are newly produced in baryon–antibaryon pairs.

There are also observables where the difference between the two versions of the model are rather insignificant. Examples are the average transverse momentum of charged hadrons as function of the energy and the average charged multiplicity $< n_{ch} >$ as function of the collision energy.

Acknowledgements. The work of S.R and R.E. is supported by the US Department of Energy under contracts DE–AC03–76SF00515 and DE–FG02 91ER40626, respectively.

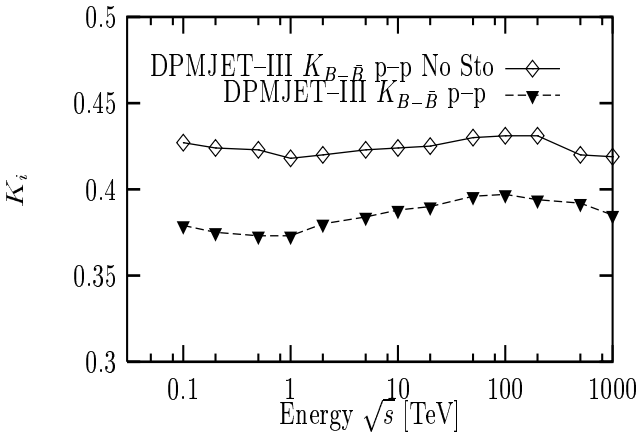

Fig. 6. Laboratory energy fractions for net baryons (baryon minus antibaryon) $B - \bar{B}$ production in p–p collisions as function of the cms energy $\sqrt{s}$.

References

D. Kharzeev, *Phys.Lett.* B 378(1996)238.

A. Capella and B. Kopeliovich, *Phys. Lett.* B381(1996)325.

J. Ranft, Baryon stopping in high energy collisions and the extrapolation of hadron production models to cosmic ray energies, Preprint *hep–ph/0002137*, (2000).

T. Alber et al., NA35 Collaboration , *Z. Phys.* C 64(1994)195.

T. Alber et al., NA35 Collaboration , *Eur. Phys. J.* C2(1998)643.

A. Capella, E. G. Ferreiro and C. A. Salgado, *Phys. Lett.* B459(1999)27.

A. Capella and C. A. Salgado, Baryon stopping and hyperon enhancement in the improved dual parton model, *hep–ph/9903414*, *preprint LPT Orsay 99–20* (1999).

S. E. Vance and M. Gyulassy, Anti–hyperon enhancement through baryon junction loops, Preprint *Cu–YP–929, nucl–th/9901009* , 1999.

J. A. Casado, *hep–ph/9810357v3, Manchester preprint MC–TH–98–17* (1999).

S. Roesler, R. Engel and J. Ranft, The event generator DPMJET–III at cosmic ray energies, presented at the same meeting.

A. Solano, HERA, by H1 and ZEUS Collaborations, *Nucl. Phys. Proc. Suppl.* 82(2000)36.

B.B. Bach et al. PHOBOS Collaboration, *Phys.Rev.Lett.* 85(2000)3100.

K. Adcox et al. PHENIX Collaboration, nucl–ex/0012008 (2000).

G. Roland PHOBOS Collaboration, presented at Quark Matter 2001 Meeting (2001).

I.G. Bearden, BRAHMS Collaboration, presented at Quark Matter 2001 Meeting (2001).

H.Z. Huang, STAR Collaboration, presented at Quark Matter 2001 Meeting (2001).

H. Ohnishi, PHENIX Collaboration, presented at Quark Matter 2001 Meeting (2001).

T.K. Gaisser, *Cosmic Rays and Particle Physics*, Cambridge University Press, 1990.